CHAPTER 4

Evaluation of NPS Return Flow to the River Using a Water Balance Model

4.1. Water Balance Model Applied to the LARV

Water Balance Model Equation.

The purpose of the water balance model is to determine the volume of unaccounted for water in each reach. We begin with a basic water balance model as describe in most hydrology texts — (Wanielista, Kersten, Eaglin, et al. 1997).

change in storage = inputs - outputs

Adding the variables, both known and unknown, present in the LARV we have the following equation:

$$\frac{\Delta S}{\Delta t} = Q_{in,US} + \sum Q_{in} + P + R + B - Q_{out,DS} - \sum Q_{out} - E - T - F \qquad (1)$$

Where:

$\frac{\Delta S}{\Delta t}$ = Stored volume change between time steps.

$Q_{in,US}$ = Flow in the river entering the study reach at the upstream end.

$\sum Q_{in}$ = Flow gained by the river from tributaries and other gauged sources.

P = Volume of water gained to the river due to precipitation falling directly on the river's surface.

R = Volume of water gained to the river due to precipitation runoff from adjacent land.

B = Volume of water gained to the river due to subsurface flow.

$Q_{out,DS}$ = Flow in the river leaving the study reach at the downstream end.

$\sum Q_{out}$ Flow lost from the river to canals and other gauged sinks.

E = Volume of water lost from the river due to direct evaporation from the water's surface.

T = Volume of water lost from the river due to plant transpiration.

F = Volume of water lost from the river due to infiltration into the subsurface flow.

If we combine the terms that are unknown or unmeasured, we arrive at the following equation:

$$\frac{\Delta S}{\Delta t} = Q_{in,US} + \sum Q_{in} + P - Q_{out,DS} - \sum Q_{out} - E + Q_{NPS} \tag{2}$$

Where:

Q_{UNPS}= The sum of gains from non-point sources and losses to non-point sinks ($Q_{NPS} = R + B - T - F + Q_{U,in} - Q_{U,out}$).

There is no reasonable method for differentiating the components of Q_{UNPS}, therefore the abbreviation NPS in this thesis refers to both non-point sources and non-point sinks. Q_{UNPS}includes the non-point source gains from groundwater sources(B), non-point source losses to groundwater sinks F), transpiration losses from plants in the river channel (T), and gains from precipitation runoff from adjacent land (R). Additionally, this term includes ungauged flows leaving and entering the river. Ungauged gains to the river ($Q_{U,in}$) are suspected to be primarily in the form of irrigation drainage from adjacent farmland. Other sources could be due to errors in underestimating flows entering the river or overestimating flows leaving the river. Ungauged losses from the river ($Q_{U,out}$) are suspected to be primarily in the form of minor or unauthorized withdrawals from the river channel. Of the

ungauged flows, irrigation drainage from adjacent farmlands is assumed to be the largest contributor.

The two groundwater components of $Q_{UNPS}$are suspected of being the largest components of Q_{UNPS}. Water transfer between the aquifer and river happens continually whereas $Q_{U,in}$, $Q_{U,out}$, R, and T are not continuous. $Q_{U,in}$ and $Q_{U,out}$ only occur periodically when individuals actively withdraw from the river or allow irrigation runoff to return to the river. R only occurs during rain events. Within the LARV, most rainwater is captured in irrigation canals. Only precipitation falling in the riparian zone is likely to reach the river. T only occurs during growing season. This value is also only considering the transpiration happening within the river channel and does not include the riparian zone. Any losses due to transpiration in the riparian zone are first considered river losses to the aquifer (F).

Re-arranging equation (2) to solve for the unknown values produces equation 3. Due to the nearly identical method of calculating flow (Q) and it's associated error and uncertainty, these terms were associated with each other. Likewise, the precipitation (P) and evaporation (E) terms were associated with each other.

$$Q_{UNPS} = \left(Q_{out,DS} + \sum Q_{out} - Q_{in,US} - \sum Q_{in}\right) - \frac{\Delta S}{\Delta t} - (P + E) \tag{3}$$

A time step of one day was established for all models calculated in this thesis. Most of the data from agencies is readily available in average daily format. While most of the data could also be obtained in hourly or quarter-hourly format, it was assumed that the additional information would not improve model accuracy.

4.2. Stochastic and Deterministic Models

Deterministic and stochastic models are used in both the unaccounted for water and mass balance models. Deterministic models are fully determined by the input parameters or variables. Randomness of any kind is not included. Stochastic models extend deterministic models by including one or more random parameters. Given the same input parameter values, a stochastic model will produce different results with each iteration.

There are many recognized methods for solving stochastic models. Solutions to these models are not definite and the term "solve" must be taken loosely. Any individual solution from a stochastic model is one of a potentially infinite number of possible solutions. The Monte Carlo (MC) simulation technique was used to obtain solutions for all stochastic models in this thesis. The MC technique is conceptually simple. The stochastic model is repetitively solved in a series of iterations. The combined solutions from all iterations are used to define the solution statistics of the model.

The number of iterations performed is determined in a number of ways. One way is to calculate a set of identifier statistic(s) after each run. Identifier statistic(s) are those that the modeler has determined to be of value in determining when to terminate the model. Usually, these statistics are monitored to identify when the change in the statistic has reached a predetermined threshold. An alternate method of determining the number of iterations to perform is more fixed. The model is run for a estimated number of iterations. A set of results for each iteration is saved. After all iterations are calculated the identifier statistic(s) are calculated for each iteration. The modeler then determines the number of iterations based on the results. The modeler must determine the best method based on a number of factors to include software and hardware limitations and the limits of the modeler's programming skills.

It was determined that for the sake of simplicity, all of the models calculated in this thesis would use the same number of iterations. The USR mass balance model is the most complex model as it has the largest number of input variables and uncertainty terms. The identifier statistics used were the mean, variance, and skewness, which are the first, second, and third moments of the probability density. These were calculated for each iteration. The threshold between the observed iteration and the previous iteration was fixed at 0.1%. The identifier statistics reached the threshold in the following order: mean, variance, and skewness. Skewness reached its break point shortly before the 500th iteration. A judgment call was made to increase the factor of safety. Therefore, the number of stochastic model iterations was fixed at 5,000.

4.3. Error and Uncertainty.

Any problem that measures variable natural processes must account for parameter and model uncertainties (Vicens, Rodríguez-Iturbe, and Schaake 1975). Parameter uncertainty is derived from measurement error, spatial variability, and temporal variability (Herschy 2002). Measurement error is the difference between the true and measured values. Most of this error type is due to instrument measurement inaccuracies due to either error inherent in the instrument or from errors in calibration or measurement. Measurement errors inherent to the instrument are uncorrectable and cannot be accounted for within the model. Errors due to calibration or measurement deviations are only correctable at the time of measurement or calibration and cannot be accounted for within the model.

Spatial variability is the difference in the true value at different points when measured at the same time. Data collected at a single given point in space may not be representative of the area it is assumed to represent due to spatial variability. This can manifest itself even

with very small distances between measurements. Temporal variability is the difference in the true value at the same point, but at different times. Data collected at a one time may not be representative of the time frame it is assumed to represent due to temporal variability (Gates and Al-Zahrani 1996). Again, this can be manifested even over small time differences. Due to instrument error, the spatiotemporal variability of the measured object, and the inability to know the true value of the measurement, reported parameter values should be treated as random variables (C. T. Haan 1989; Charles Thomas Haan 2002).

Almost all of the data was obtained from outside agencies and was not collected by the research team. These agencies have data uncertainty ranges that account for all parameter uncertainties. These uncertainties are expressed in accordance with the ISO Guide to Expression of Uncertainty in Measurement (GUM) (ISO 2008). While the GUM classifies uncertainty as either "Type A" or "Type B", the all of the data included in this thesis has uncertainty evaluations described as "Type B". Type B evaluations usually use standard deviations and assumed probability distributions obtained from scientific judgment, available information, and possible variability of a measurement.

For most of the data used in this thesis, we are not the data originators. The data originators have provided uncertainty ranges which include instrument measurement random error and uncertainties due to temporal variations of the measured location. The root mean square method is used to estimate the uncertainty related to measurement of water quantity and water quality values (Harmel and Smith 2007; ISO 2008). Harmel and Smith (2007) describe this measurement uncertainty as the probably error range, and quantify upper and lower uncertainty boundaries for measured data points as the following when attempting to specify an expected range of expected values.

$$\sigma^2 = \left(\frac{O_i - UO_i(l)}{3.9}\right)^2 \qquad or \qquad \sigma^2 = \left(\frac{UO_i(u) - O_i}{3.9}\right)^2 \tag{4}$$

Where:

$\sigma^2 =$ variance about measured data value O_i.

$O_i =$ measured value.

$UO_i =$ upper (u) and lower (l) uncertainty boundaries.

$3.9 =$ number of standard deviations accounting for $> 99.99\%$ of a normal probability distribution

The data collected for this thesis is assumed to represent the mean of a normal distribution of possible values. The upper and lower bounds of the distributions are given as either a percent or value deviation from the mean. Equation 4 is re-written from the definition found in Harmel and Smith (2007) to that found in equation 5.

$$\sigma^2 = \left(\frac{\mu - (\mu - \mu p)}{3.9}\right)^2 \qquad or \qquad \sigma^2 = \left(\frac{(\mu + \mu p) - \mu}{3.9}\right)^2 \tag{5}$$

Where:

$\mu =$ the reported value (assumed to be the mean).

$p =$ the reported percent deviation from μ.

Both of these equations in 5 simplify to equation 6. The standard deviation is shown as the calculated result due to the requirements of the calculating software.

$$\sigma = \frac{\mu p}{3.9} \tag{6}$$

When the upper and lower bounds are defined as a value deviation from the reported value, then equation 4 becomes:

$$\sigma^2 = \left(\frac{\mu - (\mu - v)}{3.9}\right)^2 \qquad or \qquad \sigma^2 = \left(\frac{(\mu + v) - \mu}{3.9}\right)^2 \tag{7}$$

Where:

$v =$ the reported value deviation from μ.

In this case, both equations in 7 simplify to:

$$\sigma = \frac{v}{3.9} \tag{8}$$

The difference between a model's calculated or estimated value and the reported value is called a residual. The distribution of residuals is the model uncertainty. These distributions are uni-variate and do not have predefined shapes. There are a variety of statistical and graphical tools available to analyze unknown residual distributions to determine a best fit parametric distribution. The two graphical tools used in this thesis are the histogram and the kernel density plot.

Non-parametric distribution models are used as an aid for analyzing uni-variate data sets. Specifically, kernel density estimates (KDE) are used in conjunction with histograms

to assist in visual analysis of the data. Figure 4.1 is an example of a random sample of one of the input data sets used in this thesis. The curve is the KDE. The short vertical lines between the histogram and the x-axis, called a rug, depict the data values. This figure adequately displays the resulting differences between histograms and KDE. KDEs can more accurately depict data groupings that are lost in histogram bins. The histogram leads us to believe that the data has a strong tendency to be near zero, wile the KDE shows that the majority of the data is between 0-20. Histograms can more accurately depict extremes or cut-off values. In the figure, there are no values less than zero. The histogram clearly shows this while the KDE shows that there are values less than zero. Both histograms and KDE are used throughout this thesis to assist in the description of distributions. A rug is also presented with the histogram whenever the quantity of data allows for adequate data presentation. A rug is not included when the data set is too large to allow for discreet identification of data values.

Determining which parametric distribution best fits the uni-variate residual distribution requires the use of both the graphical and statistical tools. For each residual distribution, probable parametric distributions types were chosen for testing against the residual distribution. For each of these parametric distribution types, a best fit was generated using the maximum likely-hood estimator (MLE) method. These MLE results were then analyzed using Kolmogorov-Smirnov (K-S), Cramer-von Mises (CvM), and Anderson-Darling (A-D) goodness-of-fit tests to determine which distribution type best fit the uni-variate residual distribution. All three tests are non-parametric tests of continious uni-variate probability distributions. The K-S and CvM tests calculate the difference between the empirical cumulative density function (ECDF) of the test data and the cumulative density function (CDF) of the tested reference distribution. The K-S and CvM tests use different algorithms to perform

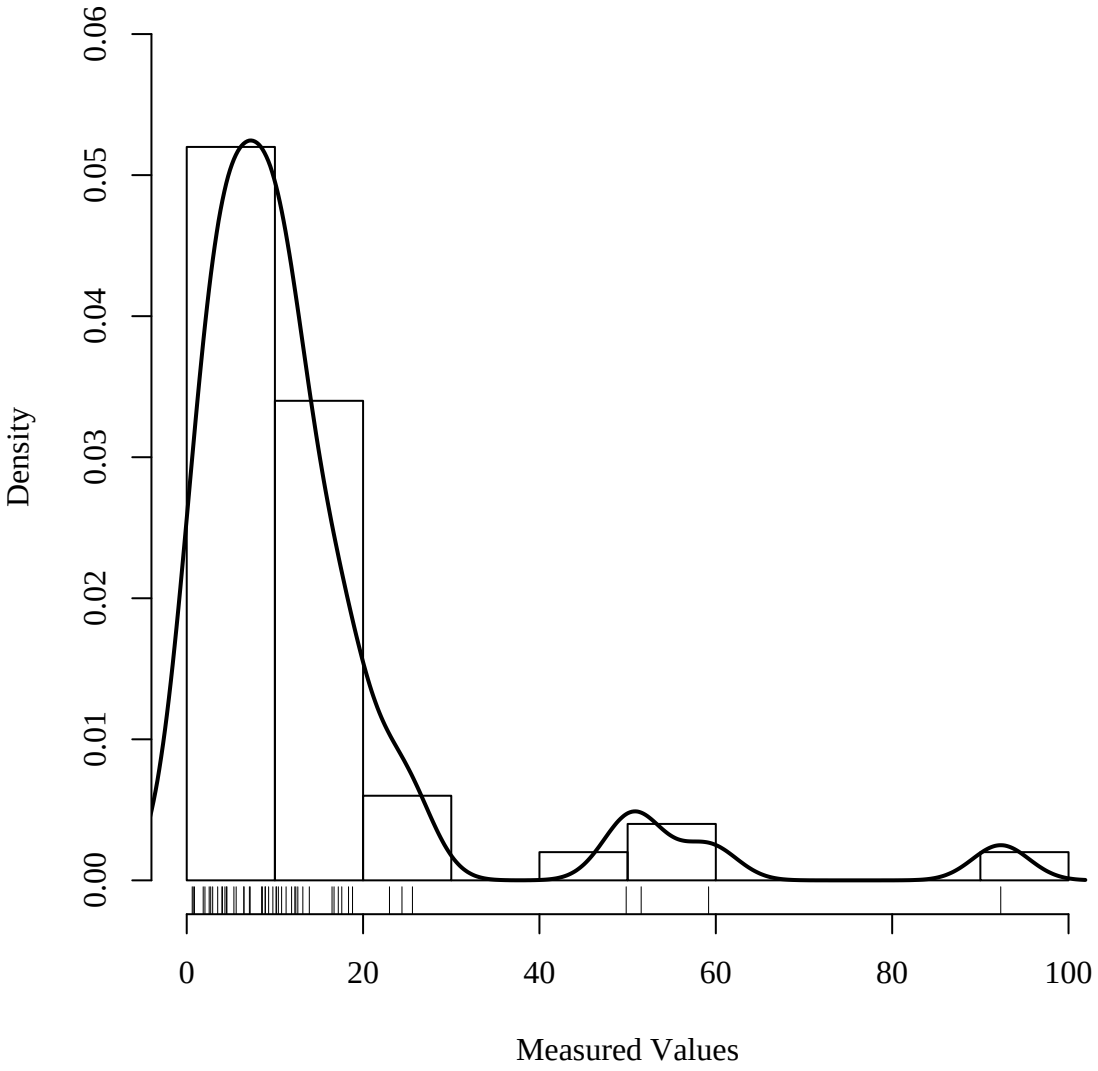

Figure 4.1. Example kernel density estimate. The data is a random sample of an input variable used in this thesis. The curve depicts the kernel density estimate. The short vertical lines between the histogram and the x-axis, called a rug, depict the data values.

the calculation. Each of the goodness-of-fit tests has their own strength and weaknesses and as such, graphical tools are used to confirm or refute the statistical test results (D'Agostino and Stephens 1986; Delignette-Muller and Dutang 2014; Venables and Ripley 2002).

4.4. River Storage Change

River reach estimated stored water volume changes ($\frac{\Delta S}{\Delta t}$) from equation 1 are the sum of the river segment stored water volume changes for each reach (Equation 9). The storage change for each segment is calculated independent of adjacent segments.

$$\frac{\Delta S}{\Delta t} = \sum \frac{\Delta S_i}{\Delta t} \tag{9}$$

Where:

$\Delta S =$ Water storage change in the river reach.

$\Delta S_i =$ Water storage change in river segment i.

$\Delta t =$ Model time step = 1 day.

River reach volume changes are calculated between two consecutive time steps. Reach volume changes are calculated as the sum of the volume changes within the segments that compose the reach. River segment volume change between time steps is calculated as shown in equation 10.

$$\frac{\Delta S_i}{\Delta t} = L_i \cdot \frac{\Delta A_i}{\Delta t} \tag{10}$$

Where:

$\frac{\Delta S_i}{\Delta t}$ = Segment storage change.

L_i = Segment length.

$\frac{\Delta A_i}{\Delta t}$ = Segment cross-section area change.

Figure 4.2 shows the difference between a simplified example of a natural channel and the modeled channel. Although the river is variable in width and depth along its entire lengths, it is modeled as a trapezoidal prism with a constant length and with a cross-section

that does not vary with respect to location. It was reasoned that this simplistic model would best approximate the average channel shape along the entire reach. The channel water surface elevation is assumed to be constant through each segment. This assumption is not true in nature, but we are not concerned with the water surface elevation, but with the flow depth. We are assuming that the flow depth remains relatively constant through a river segment. This assumption assumes that all gains and losses to the river are accounted for either through flow gains and losses, evaporation, precipitation, or unaccounted for gains and losses as shown in equation 1.

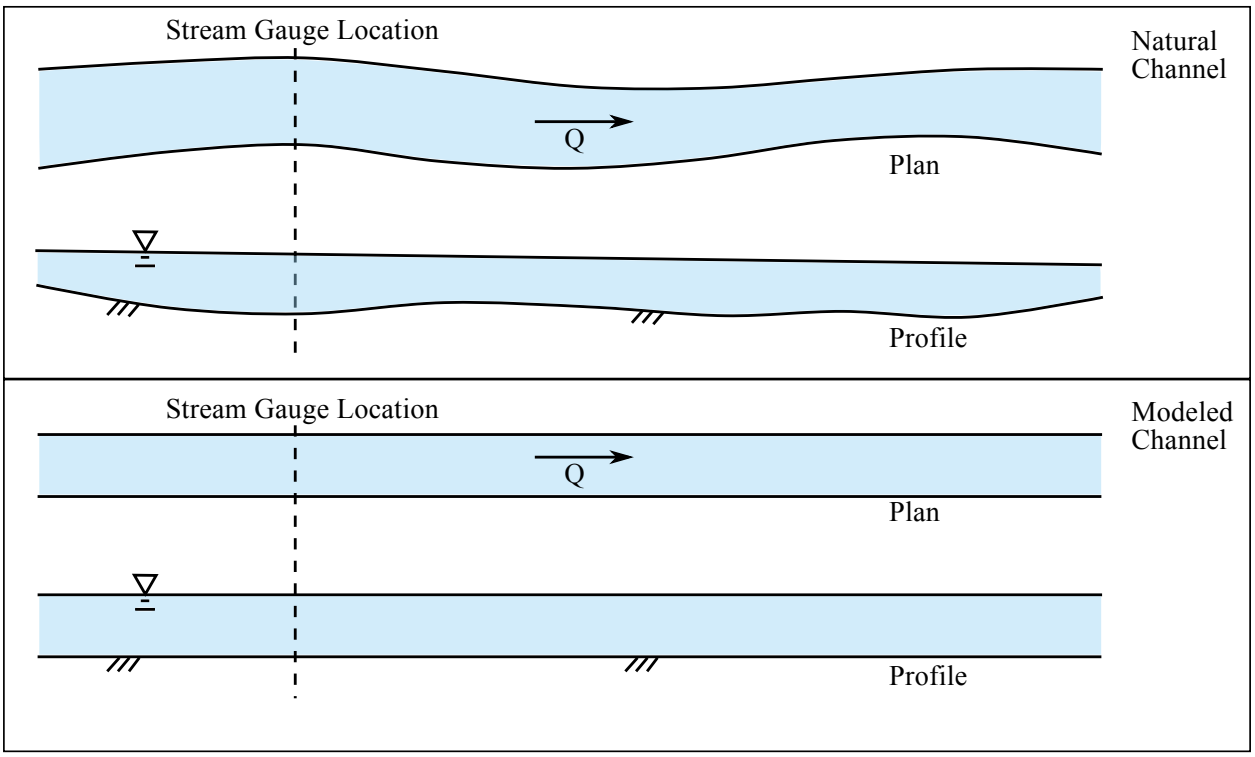

Figure 4.2. River Segment Model.

Segment lengths, as reported in Table 4.2, are sufficiently short such that any surges due to irrigation canal gates changes, precipitation events, or other events pass through the segment in less than a day. The total travel time in the USR is 2-3 days and 1-2 days in the DSR based on USGS reported average stream velocity measurements taken in

conjunction with stream gauge calibrations. River segment length (L_i) was measured to the nearest 0.1 km using publicly available satellite imagery, USGS hydrography data, and geographical information system (GIS) software. River segment length was calculated as the length of the thalweg between the segment endpoints. When the USGS thalweg did not follow along the river channel as shown in the satellite imagery, a new thalweg was drawn. Rough validation of these measurements was performed in the field by comparing the GIS calculated length of adjacent roadways to the actual driven distance as reported by a vehicle odometer. River lengths are assumed to be constant throughout the study time frame. Individual and combined variations in the channel path along a river segment were assumed to be negligible.

Table 4.2. River Segment Lengths.

Study Reach	River Segment	Segment Length km	Segment Length mi
USR	A	12.5	7.8
	B	3.9	2.4
	C	30.7	19.1
	D	37.8	23.5
	E	14.3	8.9
DSR	F	37.6	23.4
	G	24.9	15.5

River segment cross-sectional area change $\left(\frac{\Delta A_i}{\Delta t}\right)$ calculation is based on the trapezoidal area that approximates the difference between the cross-sectional area at two different flow depths as depicted in Figures 4.3 4.4 and in equation 11. While the cross sectional area difference isn't exactly a trapezoid, the difference for small differences in gauge height is insignificant. Figure 4.3 shows a simplified river cross section at a stream gauge location. As previously discussed, stream gauges do not hold the channel bottom as their datum.

They have an arbitrarily fixed datum that does not move unless determined by the gauge owner.

The difference between the stream gauge datum and the channel bottom is corrected using a constant correction factor calculated from the river survey. The gauge datum does not have a known marker where the elevation could be directly measured. Instead, the surveyed water surface elevation was recorded at the gauge location on both sides of the channel. The flow depth value was calculated by finding the difference between the surveyed average water surface elevation and the surveyed channel bottom elevation. The flow depth was then compared to the stream gauge height reported for the same date and time as when the water surface elevation was surveyed. The difference between the reported value and the average of the surveyed values was taken as the correction factor for the gauge. This procedure was repeated for each gauge.

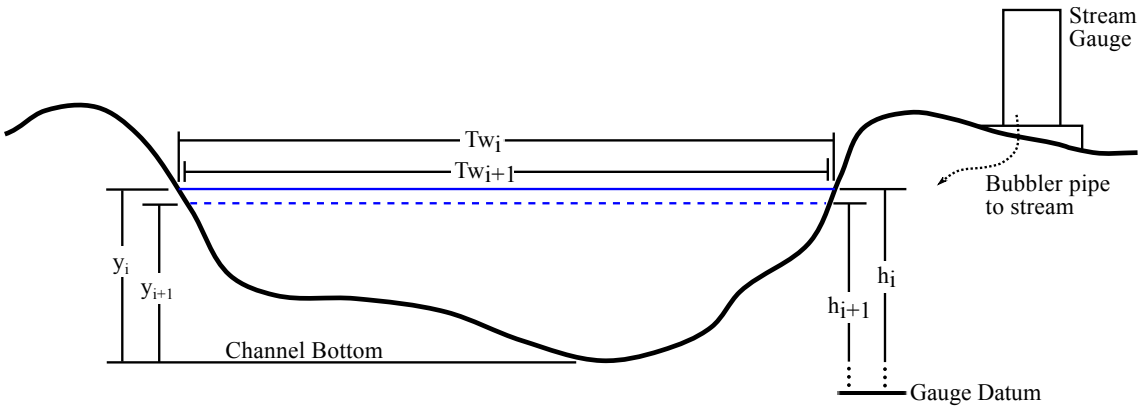

Figure 4.3. Average river segment cross-section area change.

$$\begin{aligned}\frac{\Delta A_i}{\Delta t} &= \overline{Tw} \cdot \Delta y \\ \frac{\Delta A_i}{\Delta t} &= \frac{Tw_t + Tw_{t-1}}{2} \cdot (y_{t-1} - y_t)\end{aligned} \tag{11}$$

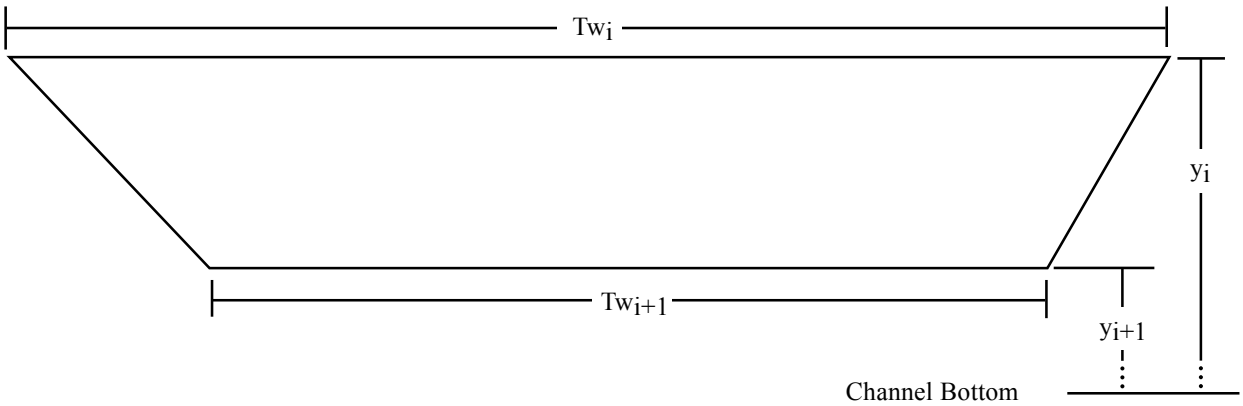

Figure 4.4. River cross-section area change diagram.

Where:

$_t$ = Current time step.

$_{t-1}$ = Previous time step.

$\frac{\Delta A_i}{\Delta t}$ = Cross-section area change at river section i between time steps.

$\overline{Tw}$ = Average river top width.

Δy = Change in flow depth from the previous time step.

Tw = River top width.

y = River flow depth.

Flow depth values as reported by the USGS and CDWR are measured values with an associated probability range as calculated in equation 6. The uncertainties are applied as shown in equation 12. A correction factor (C_i) is applied to each reported gauge depth to correct for the difference between the gauge datum and the channel bottom as measured during the channel cross-section survey. Two separate uncertainties are applied. ε_{h1} is the uncertainty distribution as described by the gauge owner. This uncertainty is reported by both the USGS and CDWR as being normally distributed with extreme values at ± 0.01 ft

($\pm 0.003\,\mathrm{m}$) (Cobb 1989). The second uncertainty term, ε_{h2}, is the result of personal observation of the river channel along its entire length. This term describes the variability in flow depth. It was observed that the channel depth did not vary greatly along most of its length. There were particular areas where there were deeper pools, but these areas were noted to be more prone to ponding during low flow. It is assumed that the average effective flow depth only varies within a normal distribution with limits of $\pm 0.076\,\mathrm{m}$ ($\pm 0.25\,\mathrm{ft}$). There is the possibility that ε_{h1} could cause the storage change between the time steps to change from a storage gain to a storage loss, or vise versa. This is acceptable as it is within the measurement limits of the instruments. Once $h + \varepsilon_{h1}$ has been calculated for the two successive time steps, the relationship between the two time steps is fixed. If the river segment flow depth rises between time steps after this calculation, then that relationship must continue throughout the rest of the calculation for V_x. To facilitate this, it is assumed that ε_{h2} does not vary significantly within the study time frame and does not vary within a realization. The Arkansas R. channel is sufficiently stable between consecutive days that this assumption is valid. A new ε_{h2} is drawn for each realization and remains constant for all time steps within the study time frame.

$$y_{i,t} = h_{i,t} + C_i + \varepsilon_{h1} + \varepsilon_{h2} \tag{12}$$

Where:

$y_{i,t}$ = Section i modeled average daily flow depth at time t.

$h_{i,t}$ = Section i reported average daily river gauge height at time t.

C_i = Section i river gauge height to flow depth correction term.

ε_{h1} = Reported river gauge height data uncertainty.

ε_{h2} = Estimated flow depth uncertainty.

PRESENT RIVER SEGMENT FLOW DEPTH RESULTS

River top width (Tw) is calculated using equation 13. (Buhman, Gates, and Watson 2002; Gates and Al-Zahrani 1996). The river channel does not have a fixed cross-section along it's length, therefore, the fitting parameters, β_1 and β_2 are not constant, but are from distributions of β_1 and β_2. Equation 13 and the data from each survey cross-section was used to calculate a best fit equation using non-linear regression. The β_1 and β_2 values from each cross-section were combined to determine the distribution of β_1 and β_2. The best fit distributions for β_1 and β_2 are presented in table 4.3. β_1 and β_2 values were analyzed for correlation. It was found to be insignificant with a Pearson R value of 0.17. Visual analysis of the data points showed that there was no distinguishable pattern. Future surveys will expand the data set and may show that there is a correlation between β_1 and β_2, but the available data does not support that conclusion. Also presented in this table is the best fit distribution for the residuals. These distributions and the distributions for β_1 and β_2 were analyzed to determine the best fit distribution using the methodology described in Section 4.3.

justify

$$Tw_{i,t} = \beta_1 y_{i,t}^{\beta_2} + \varepsilon_{Tw} \tag{13}$$

Where:

$Tw_{i,t}$ = River segment i average daily top width at time step t.

$y_{i,t}$ = Calculated segment i average daily flow depth at time step t calculated using equation 12.

β_1 and β_2 = fitting parameter distributions.

ε_{Tw}= Calculated average daily flow depth uncertainty.

Table 4.3. River top width fitting parameter distributions.

Study	Fitting	Best Fit Distribution		
Reach	Parameter	Dist. Shape	p1*	p2*
USR	β_1	logistic	16.8	7.53
	β_2	log-normal	-1.27	1.57
	Residual	logistic	1.99	0.99
DSR	β_1	logistic	28.2	4.84
	β_2	log-normal	-0.43	0.65
	Residual	log-normal	0.87	0.57

* Distribution fitting parameters. For logistic, p1=location and p2=scale. For log-normal, p1=mean of the log scale and p2=standard dev. of the log scale

Non-linear regression models are those models where the function of the predictor variable, f_i, contains a fitting parameter, β_i. Non-linear regression models were used only when a specific model form could be determined from known physical or geometrical relationships. R-squared values were not used to determine goodness-of-fit for non-linear regression models. These models can have valid values that are negative or greater than one (Spiess and Neumeyer 2010) and as such are outside of the boundary for comparing linear models. Pseudo or modified r-squared calculations are available. These computations result in values

that are comparable to the r-squared value for linear models, but have slightly different interpretations . Since non-linear regression models were used only when specific model forms could be predetermined, there was no need to compare different model forms estimating the same result.

reference

Goodness-of-fit for non-linear regressions used in this theses are purely for informational purposes. Since all non-linear models were based on known relationships, goodness-of-fit values only serve to show how well the data fits the model. In order to define non-linear regression model goodness-of-fit, the root mean squared error (RMSE) value was calculated. The RMSE represents the standard deviation of the differences between he predicted and observed values. The RMSE is scale dependent as the units are the same as the observed value. The RMSE is also known as the standard deviation. This would cause an issue if models for different observed value units and scales were compared against each other. In this study, non-linear regression models are only used to estimate the cross-sectional width of a river segment and to estimate the selenium concentration at one location. Since all cross-section analyses use the same measurement units, this allows us to compare the residual errors associated with the various cross sections without needing to consider scale or units.

Values β_1 and β_2 are drawn from probability distributions. Calculated flow depth and river top width data pairs were used to determine the distributions from which β_1 and β_2 in equation 13 were drawn. These distributions were developed using non-linear, least-squares regression. Values below 0.15 m (0.5 ft) were removed from the regression analysis. Flow values below this depth are not common and it was determined that these points would not allow for an accurate representation of the flow depth to river top width relationship for the range of known flow depths. Values above 1.52 m (5.0 ft) were also removed from the

regression analysis. Flow depths above this depth are above the banks of the primary river channel and are within the inner flood plain. Table 4.4 gives the resulting β_1 and β_2 values for each surveyed cross-section. Figure 4.5 is an example of the surveyed flow depth and river top width relationships and the derived non-linear relationship for cross-section 1 in river segment A of the USR. Similar relationship plots for the other surveyed cross-sections are found in the appendix.

Figure 4.6 shows the distributions of β_1 and β_2 values and the various best-fit distributions in both the USR and DSR. Logistic, normal, exponential, Weibull, and log-normal distributions were fitted to the data. Vertical tick marks in the x-axis margin are at the data values. Kernel density estimations were used as an alternative means to graphically represent the data density. Kernel density estimations are non-parametric and when paired with histograms of the same data, they are used to assist in visual data analysis and comparison to parametric density functions. The K-S goodness-of-fit statistics, presented in table 4.5, were calculated for the fitted distributions and known data.

Combining the river cross-section analyses to create single distributions of β_1 and β_2 was a necessary step as there was an insufficient number of cross-sections within each river segment to provide for a statistically significant data set. The resulting river shape parameter distributions are valid for the river segment for which they were calculated. Each river segment draws values from the shape parameter distributions independently. Only one pair of shape parameters is drawn for each realization. It is assumed that the river geometry does not significantly change within the study time frame. Channel variability is modeled between the realizations.

Residuals from the non-linear regression analyses were combined into a single data set for error analysis. Combining this data set was a logical step following the combination

Table 4.4. Arkansas River top width estimating coefficients.

Study Region	River Segment	Cross-Section	Fitting Parameter β_1	Fitting Parameter β_2	Root Mean Squared Error
USR	A	1	101.8	0.4546	11.43
		2	61.96	0.02487	0.1710
		3	77.29	0.1736	8.363
	B	4	69.40	0.06101	0.7084
		5	51.77	0.9319	1.924
		6	63.93	0.03910	2.152
	C	7	50.13	0.7839	2.562
		8	71.04	0.4024	2.900
		9	71.36	0.1684	4.719
		10	87.08	0.02590	0.5928
		11	61.49	0.09547	4.631
		12	72.67	0.5591	3.487
	D	13	45.97	0.6918	4.568
		14	45.71	0.6290	3.034
		15	86.75	0.5579	4.701
		16	20.71	0.1360	1.244
		17	51.74	0.1889	2.375
		18	27.97	0.3204	1.807
		19	36.29	0.07383	0.1955
	E	20	33.00	0.6961	1.533
		21	182.0	1.270	1.916
DSR	F	1	22.48	0.4006	0.8139
		2	41.61	1.390	3.953
		3	29.82	0.2265	1.821
		4	21.46	0.3801	2.541
		5	22.78	0.8004	5.715
		6	26.21	0.4153	1.681
		7	41.92	1.487	3.299
	G	8	23.49	1.504	2.344
		9	33.54	1.106	3.676
		10	28.03	0.5790	2.003
		11	24.16	0.2103	1.693
		12	24.74	0.8992	2.617
		13	52.68	1.1850	5.757
		14	24.18	0.4764	0.9259

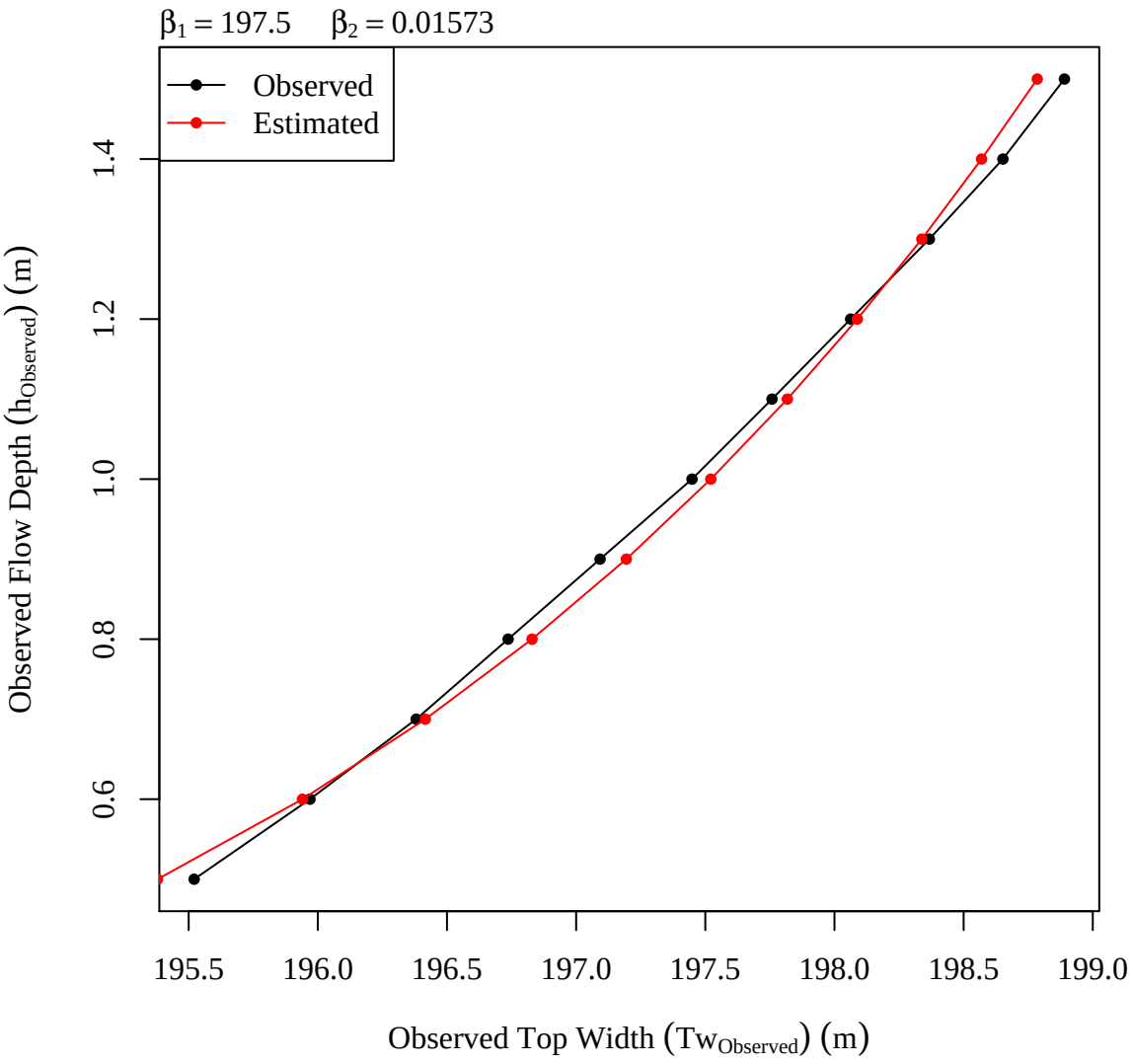

Figure 4.5. Example Flow Depth vs. River Top Width Relationship. The non-linear best fit line of the form in Equation 13 is red. The values are the two non-linear regression fitting parameters (β_1 and β_2) and the residual standard error for the fitting equation (σ). Similar figures for all cross-sections are found in the appendix.

of the data that generated the residuals. Residuals were tested using the same tools and techniques used to test the river shape parameter distributions. USR and DSR channel shape residuals were found to have a log-normal distribution. Figure 4.7 presents the distribution analyses for the USR and DSR. These figures are of the same type as those used to analyze the river shape parameter distributions, figure 4.6.

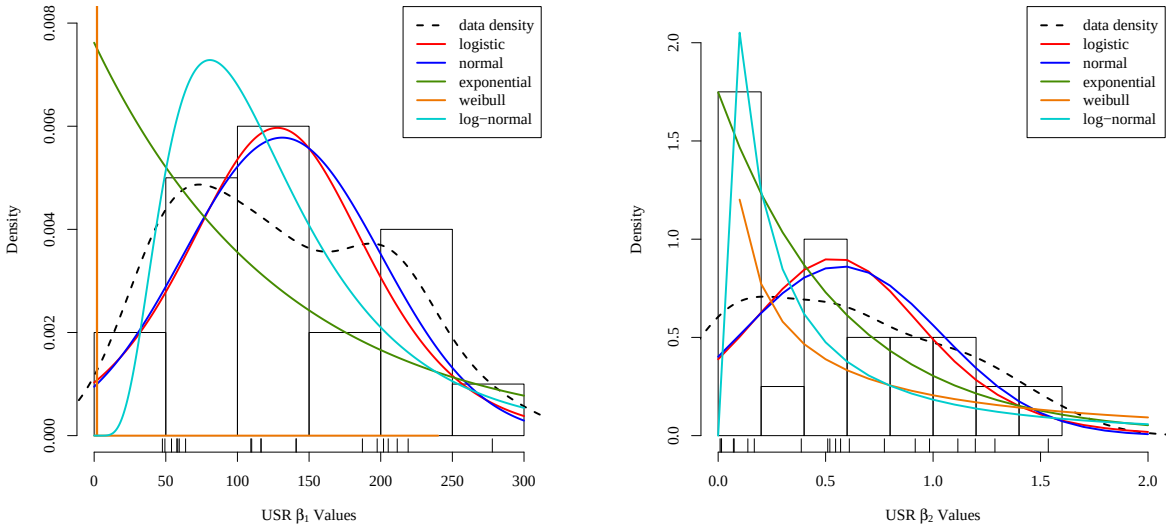

(a) USR β_1 **(b)** USR β_2

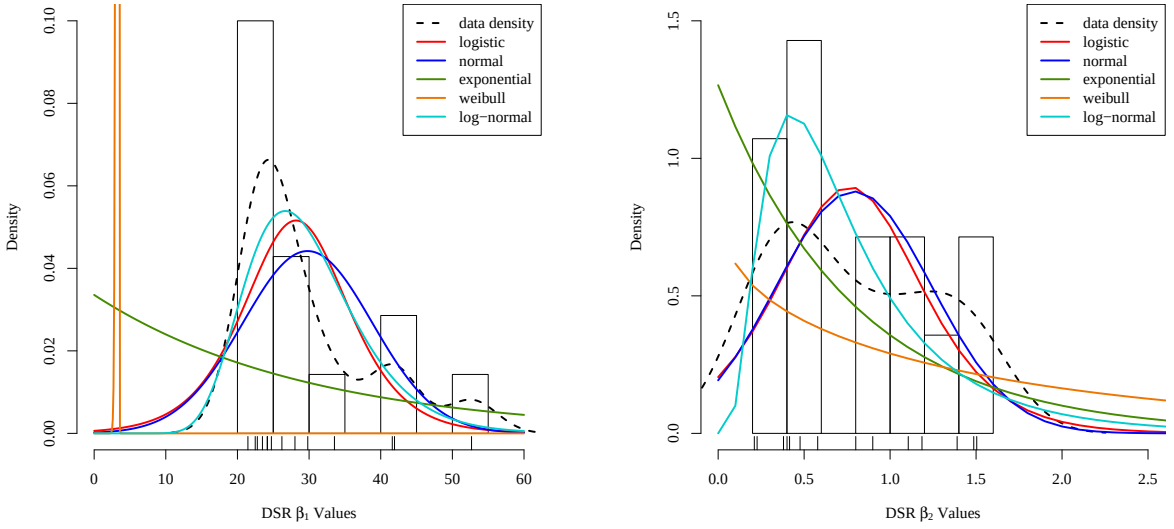

(c) DSR β_1 **(d)** DSR β_2

Figure 4.6. *Tw* Versus *h* Fitting Parameter β_1 and β_2 Distributions. The black dashed line is a kernel density plot representing a histogram where the bin size approaches zero. The colored curves are the best fit for the particular distribution type. Vertical tick marks in the x-axis are at the data values.

Residuals are the collection of the difference between the calculated regression model values and the measured values. Collectively, the distribution of the residuals describe the uncertainty of the regression model. In this case, the distribution of residuals describe the top width estimating uncertainty ε_{Tw}. Residuals should be tested for heteroskedasticity

Table 4.5. River β_1 and β_2 distribution test results.

Fitting parameter	Distribution	K-S Statistic
USR β_1	Logistic	0.1211
	Normal	0.2092
	Exponential	0.3178
	Weibull	1.0000
	Log-normal	0.1236
USR β_2	Logistic	0.1837
	Normal	0.2040
	Exponential	0.1379
	Weibull	0.3412
	Log-normal	0.1570
DSR β_1	Logistic	0.1999
	Normal	0.2258
	Exponential	0.5134
	Weibull	1.0000
	Log-normal	0.2086
DSR β_2	Logistic	0.1657
	Normal	0.1839
	Exponential	0.2391
	Weibull	0.4326
	Log-normal	0.1486

to determine if the model does not adequately predict the data. Heteroskedasticity is the condition where the variability of a variable, in this case the residuals, is unequal across the range of the values and is usually. There are many tests for heteroskedasticity, but the most powerful is visual analysis of the plot of the residuals against the fitted, or calculated, values. When a small number of values is used to perform the regression, visual and computational analysis becomes difficult since patterns may appear that don't truly exist or patterns may not appear where they do exist. When heteroskedasticity was evident during model creation, the model was modified to remove the heteroskedasticity. Other methods are available to account for heteroskedasticity, but the most strongly recommended is model modification. Determining the parametric distribution that best fits the regressions is performed using the

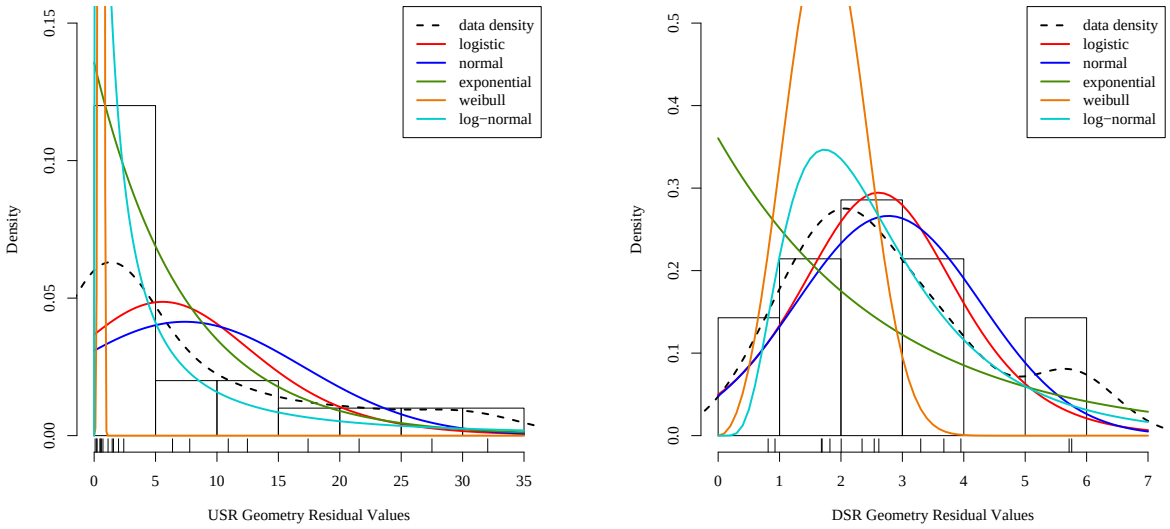

(a) USR Residuals **(b)** DSR Residuals

Figure 4.7. *Tw* versus *H* Residuals Distribution. The black dashed line is a kernel density plot representing a histogram where the bin size approaches zero. The colored curves are the best fit for the particular distribution type. Vertical tick marks in the x-axis are at the data values.

method described in section 4.3. Both visual and goodness-of-fit tests were applied to all residual regression analyses.

River segment B in the USR does not have a flow gauge within its boundaries and therefore has no reported flow depths. This segment has an additional irrigation diversion check structure within its boundaries, thereby sub-dividing segment B into two sub-segments, each with its own ungauged flow depth. Due to segment B being the shortest, composing only 3.9% of the USR's total length, and the additional variability of the possible flow depth, the average daily flow depth within segment B is taken as the mean of the reported flow depths in segment A and C. Top width and volume change calculation follows the previously described methodology.

Table 4.6. USGS Measured Field Parameter Accuracy Rating Table. This table was taken from the USGS annual water data report.

Measured field parameter	**Ratings of accuracy (Based on combined fouling and calibration drift corrections applied to the record)**			
	Excellent	**Good**	**Fair**	**Poor**
Water temperature	≤ ± 0.2 °C	> ± 0.2 - 0.5 °C	> ± 0.5 - 0.8 °C	> ± 0.8 °C
Specific conductance	≤ ± 3%	> ± 3 - 10%	> ± 10 - 15%	> ± 15%
Dissolved oxygen	≤ ± 0.3 mg/L or ≤ ± 5%, whichever is greater	> ± 0.3 - 0.5 mg/L or > ± 5 - 10%, whichever is greater	> ± 0.5 - 0.8 mg/L or > ± 10 - 15%, whichever is greater	> ± 0.8 mg/L or > ± 15%, whichever is greater
pH	≤ ± 0.2 units	> ± 0.2 - 0.5 units	> ± 0.5 - 0.8 units	> ± 0.8 units
Turbidity	≤ ± 0.5 turbidity units or ≤ ± 5%, whichever is greater	> ± 0.5 - 1.0 turbidity units or > ± 5 - 10%, whichever is greater	> ± 1.0 - 1.5 turbidity units or > ± 10 - 15%, whichever is greater	> ± 1.5 turbidity units or > ± 15%, whichever is greater

References

Buhman, Daniel L., Timmothy K. Gates, and Chester C. Watson (2002). "Stochastic Variability of Fluvial Hydraulic Geometry: Mississippi and Red Rivers." In: *Journal of Hydraulic Engineering* 128.4, pp. 426–437.

Cobb, Ernest D. (1989). *Programs and Plans–Policy Statement on Stage Accuracy.* USGS. URL: `http://water.usgs.gov/admin/memo/SW/sw89.08.html`.

D'Agostino, Ralph B. and Michael A. Stephens, eds. (1986). *Goodness-of-fit-techniques (Statistics: a Series of Textbooks and Monographs, Vol. 68)*. 1st ed. Dekker. ISBN: 9780824774875.

Delignette-Muller, Marie Laure and Christophe Dutang (2014). "fitdistrplus: An R Package for Fitting Distributions." In:

Gates, Timmothy K. and Muhammad A. Al-Zahrani (1996). "Spatiotemporal Stochastic Open-Channel Flow. I: Model And Its Parameter Data." In: *Journal of Hydraulic Engineering* 122.11, pp. 641–651.

Haan, C. T. (1989). "Parametric Uncertainty in Hydrologic Modeling." In: *Transactions of the ASAE* 32.1, pp. 0137–0146.

Haan, Charles Thomas (2002). "Statistical methods in hydrology." In:

Harmel, R Daren and Patricia K Smith (2007). "Consideration of measurement uncertainty in the evaluation of goodness-of-fit in hydrologic and water quality modeling." In: *Journal of Hydrology* 337.3, pp. 326–336.

Herschy, RW (2002). "The uncertainty in a current meter measurement." In: *Flow Measurement and Instrumentation* 13.5, pp. 281–284.

ISO (2008). "Guide to the Expression of Uncertainty in Measurement, (1995), with Supplement 1, Evaluation of measurement data, JCGM 101: 2008." In: *Organization for Standardization, Geneva, Switzerland*.

Spiess, Andrej-Nikolai and Natalie Neumeyer (2010). "An evaluation of R2 as an inadequate measure for nonlinear models in pharmacological and biochemical research: a Monte Carlo approach." In: *BMC pharmacology* 10.1, p. 6.

Venables, William N and Brian D Ripley (2002). *Modern applied statistics with S*. Springer Science & Business Media.

Vicens, Guillermo J., Ignacio Rodríguez-Iturbe, and John C Schaake (1975). "Bayesian generation of synthetic streamflows." In: *Water Resources Research* 11.6, pp. 827–838.

Wanielista, Martin, Robert Kersten, Ron Eaglin, et al. (1997). *Hydrology: Water quantity and quality control*. John Wiley and Sons.